sustainability

Article

Influence of Phosphogypsum Waste on Rainwater Chemistry in a Highly Polluted Area with High Mortality Rates in Huelva Metropolitan Area, Spain

Manuel Contreras-Llanes [1,2], Vanessa Santos-Sánchez [1,2], Juan Alguacil [1,2,3,*,†] and Roberto Rodríguez-Pacheco [4,†]

[1] Research Group in Clinical, Environmental and Epidemiology Social Transformation (EPICAS), Department of Sociology, Social Work and Public Health, University of Huelva, 21007 Huelva, Spain; mcontreras@uhu.es (M.C.-L.); vanesasantossanchez@gmail.com (V.S.-S.)
[2] Research Centre for Natural Resources, Health and Environment (RENSMA), Faculty of Experimental Sciences, University of Huelva, 21007 Huelva, Spain
[3] Consortium for Biomedical Research in Epidemiology & Public Health (CIBER in Epidemiology & Public Health—CIBERESP), 28029 Madrid, Spain
[4] The Spanish National Research Council (CSIC), Spanish Geological and Miner Institute National Center (CN IGME), Ríos Rosas 23, 28003 Madrid, Spain; roberto.rodriguez@igme.es
* Correspondence: alguacil@uhu.es
† These authors contributed equally to this work.

Abstract: This study evaluates the impact of phosphogypsum stacks on the chemical composition of rainwater in the Huelva metropolitan area, a metal-polluted area with high cancer and heart disease mortality rates. A total of 612 rainwater samples were collected using 17 rain gauges located around the study area between January 2021 and December 2022. The pH, conductivity, major ions, and trace metals were detected in the soluble fraction of rainwater. The results revealed spatial variability in the rainwater quality. The highest values of As, Ca^{2+}, Cr, F^-, NH_4^+, Ni, PO_4^{3-}, SO_4^{2-}, Sr, and V were detected in rain-gauges near phosphogypsum stacks, exceeding the levels of pH, F^-, and Ni according to the guideline values for drinking water quality from the WHO. Additionally, other pollution sources also contributed: a regional source (marine factors: Ca^{2+}, Cl^-, K^+, Mg^{2+}, and Na^+) and a local source (chemical complexes emissions: Co, Cu, Pb, and Zn). A downward trend of most toxic metal(loid) concentrations in wet depositions was detected as the distance to the affected area increased. The findings revealed that phosphogypsum stacks are a relevant source of metal(loid)s with potentially adverse environmental and public health effects that, if replicated, could be relevant for environmental monitoring and policy making.

Keywords: Huelva; rainwater pollution; phosphogypsum; spatial variation; short-range transport; particle soluble fraction; wet deposition

check for updates

Academic Editors: Robson Andreazza and Filipe Selau Carlos

Received: 12 January 2025
Revised: 19 March 2025
Accepted: 25 March 2025
Published: 31 March 2025

Citation: Contreras-Llanes, M.; Santos-Sánchez, V.; Alguacil, J.; Rodríguez-Pacheco, R. Influence of Phosphogypsum Waste on Rainwater Chemistry in a Highly Polluted Area with High Mortality Rates in Huelva Metropolitan Area, Spain. *Sustainability* **2025**, *17*, 3102. https://doi.org/10.3390/su17073102

1. Introduction

Industrial and mining environmental pollution may induce adverse health effects, including cancer, cardiovascular diseases, and respiratory conditions [1]. The Huelva metropolitan area (SW Spain), with near 300,000 inhabitants, is located on the margin of the Odiel–Tinto Estuary. This area is acknowledged as one of the world's most severely polluted sites, primarily due to widespread industrial and mining activities [2,3]. This estuary has a high content of harmful elements, both metal(loid)s (As, Cd, Cr, Cu, F^-, Fe, NH^{4+}, Ni, P, Pb, SO_4^{2-}, and Zn) and natural radionuclides from the ^{238}U decay series, including the highly radiotoxic ^{210}Pb, ^{210}Po, and ^{226}Ra [2,3]. There is support in the international scientific literature for a deleterious effect for human heath due to environmental exposure to many of those metals [1,4]. Previous studies have revealed that the mortality rates from cancer and heart disease in Huelva city are higher for both men and women compared to the national average in Spain [4–6]. According to the Spanish National Atlas of Mortality, the city of Huelva exhibited significantly higher standardised mortality ratios between 1989 and 2014 for both men and women. These elevated ratios were observed for acute myocardial infarction, cerebrovascular diseases, bladder cancer, cardiac failure, and other cardiovascular conditions. Additionally, women experienced higher mortality rates for breast cancer, while men faced elevated mortality rates for lung cancer [7]. Furthermore, previous studies focused on the cumulated heavy metals levels (As, Cd, Cr, Cu, and Ni) in the hair and urine of children from the city of Huelva; the average levels of cadmium were found to be higher than those reported in other European research [8,9], and indicated an intellectual functioning effect in the children with high Cd concentrations [9]. Similarly, an explorative research paper linked environmental exposure to heavy metals with the cognitive behaviour of children in Huelva city [10]. In addition, industry workers of Huelva city showed elevated concentrations of arsenic and other metal(loid)s, even when accounting for seafood and fish intake [11]. Although industrial and mining pollution may be the factors that have contributed to the high mortality ratios detected in the city of Huelva [4], the issue remains uncertain. Hence, given the correlation between elevated mortality rates in Huelva city and industrial and mining pollution, along with the existence of multiple sources of exposure, it is imperative to meticulously investigate the distinct signatures of metal(loid)s specific to each pollution source. In this sense, the specific pollution signatures in marsh sediments of the Odiel–Tinto Estuary using geochemical tracers were defined by our research group [12]. In addition, we recently conducted a study that denoted the connection between the spatial variability of cumulated metal(loid)s levels in nails and exposure to pollution sources in Huelva city [13].

This scenario has incited social activism, with a primary focus on the phosphogypsum stacks, recognised as the largest Naturally Occurring Radioactive Material (NORM) waste stacks of Europe [14–16], in addition to other sources of pollution. This waste deposit is located on the highly permeable marshes just 500 m from the population [2,3]. In December 2010, judiciary authorities sanctioned the cessation of phosphogypsum stockpiling and mandated that the fertiliser company devise a restoration plan for the impacted marshlands called RESTORE 2030 (https://restore2030.com/). The Huelva City Council created a citizen participation initiative of an advisory nature and asked Huelva University to coordinate an independent committee of national scientific experts. Even though the scientific committee determined that this restoration plan was insufficient for fully restoring the affected area by the phosphogypsum stacks [17], the work has already begun.

As a consequence of the actual restoration plan and future interventions, an assessment of the environmental impact of phosphogypsum stacks in the nearby areas is necessary to monitor the impact of the restoration, encompassing, but not limited to, the effect on the Huelva metropolitan area. The restoration labours may result in resuspension of coarse particles from the phosphogypsum stacks. This occurrence could be the major source of air pollutants and could significantly affect the surrounding areas [18–20]. Industry and mining activities have a direct effect on the environment and frequently produce substantial quantities of waste containing harmful elements that reach the atmosphere [1]. Among them, fertiliser production is recognised for its significant environmental impact, as it generates a waste product known as phosphogypsum, which contains a high concentration of geo-available heavy metals and radionuclides, which are typically stockpiled, occupying large surfaces [15,16,21–23]. These areas frequently lack vegetation and are significantly affected by erosive forces such as wind and runoff water. The redistribution of contaminants in the environment is significantly influenced by particle resuspension from open-cast mining, waste dumps, and industrial activities [24–28]. Large quantities of resuspended particles, often linked to wind events, may negatively impact the health of nearby residents through various intake pathways, such as inhalation, dermal contact, and/or ingestion [24]. The dispersion of particulate matter through the atmosphere significantly contributes to environmental pollution. Air masses, moving more swiftly than water and soil masses, possess the highest capability to transport pollutants rapidly, ranging from hours to days. Wet deposition is considered one of the key methods by which air pollutants are deposited on the Earth's surface, including both toxic and non-toxic matters [29]. The chemical composition of rainwater is influenced by multiple factors, including the proximity to pollution sources, the volume of precipitation, and the movement of air masses, resulting in significant spatial and temporal variations [29]. The study of rainwater chemistry provides knowledge about its potential pollutants in order to identify and assess possible contamination sources, such as industry and mining activities, and prevent damage to natural ecosystems. Therefore, research on rainwater composition has increased in recent years around the world due to the increased recognition of the potential ecological consequences resulting from environmental pollution [29–35]. The first study, however, was conducted in the United States in the 1950s [36]. Nevertheless, studies analysing the pattern of metal(loid)s due to phosphogypsum stacks in rainwater have not been found.

Despite extensive research being performed on the rainwater quality in other highly polluted locations in Huelva province [37,38] and other research focusing on the chemical composition of Huelva city's air [39–45], the specific rainwater chemical profile in the Huelva metropolitan area has not yet been characterised in detail. Also, to our knowledge, this is the first study to analyse the impact of phosphogypsum stacks on the pH, conductivity, and chemical profile of the rainwater. Monitoring rainwater can help assess the possible effects of phosphogypsum stacks on the ecosystem. In addition, these environment risk assessments are crucial to evaluate the influence of restoration initiatives like RESTORE 2030. This study assess the distribution of the suspended pollutant particles originating from the phosphogypsum stacks to identify the radius of influence of the chemicals that have arrived via rainwater in the Huelva metropolitan area.

2. Materials and Methods

2.1. Study Area

This study was conducted using sixteen rain gauges (AD, AL, CA, CM, CO, EP, GI, JR, MO, FB, FE, PF, PI, PU, RA, and SJ) covering the Huelva metropolitan area and one in Matalascañas village (MN) within the "Doñana" National Reserve Park, an unpolluted area, all situated in Huelva province, SW Spain (Figure 1). The region experiences a Mediterranean climate influenced by the Atlantic Ocean, characterised by humid mild winters with an average temperature of 11 °C in January, and the annual precipitation is 505.6 mm. Summers are dry and warm, with an average temperature of 25 °C in August and nearly no precipitation. The geological composition of the soil is primarily made up of Palaeozoic volcanic and sedimentary rocks, which are abundant in pyrite (FeS_2) and other sulphide minerals [46].

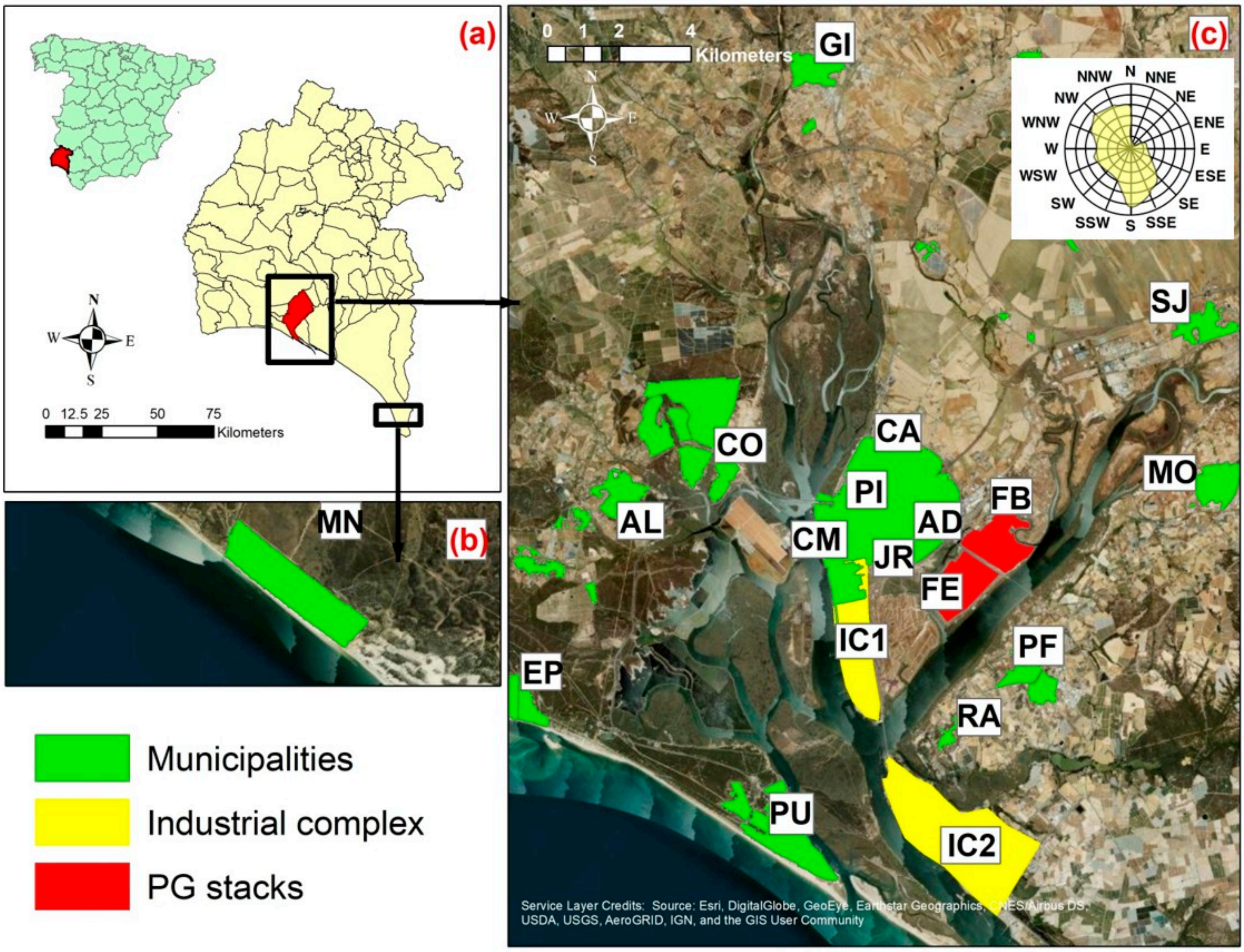

Figure 1. Location map of (**a**) Huelva province, rain gauges placed in (**b**) Matalcañas village (MN), and (**c**) Huelva metropolitan area (AD, AL, CA, CM, CO, EP, GI, JR, MO, FB, FE, PF, PI, PU, RA, and SJ) showing the wind rose diagram for the period January 2021 to December 2022. FB is the centre of phosphogypsum (PG) stacks. (IC1) Industrial complex “Polo Químico de Promoción y Desarrollo de Huelva—Punta del Sebo”. (IC2) Industrial complex “Nuevo Puerto Palos de la Frontera”.

Huelva metropolitan area, with nearly 300.000 inhabitants, is located in the Odiel–Tinto Estuary, recognised as an extremely polluted area [2,3]. A large portion of this estuary is covered by phosphogypsum stacks (Figure 1), an industrial waste product derived from phosphate rock during fertiliser production [15,16,21–23]. Over a period of 42 years (1968–2010), phosphogypsum was deposited on unconsolidated salt marsh sediments in the Tinto marshes, now encompassing 1200 hectares and containing 100 million tonnes, making it one of the most substantial deposits globally [15,16,21–23]. These phosphogypsum stacks harbour a diverse array of contaminants, including organic substances, metal(loid)s, and other harmful elements (As, Cd, Cr, F^{-}, Fe, NH^{4+}, Ni, P, Pb, SO$_4^{2-}$, and Zn). Additionally, they contain natural radionuclides from the ^{238}U decay series, including the highly radiotoxic ^{210}Pb, ^{210}Po, and ^{226}Ra [13,14,19–21], which have been linked to health problems [47]. Phosphogypsum is designated as a naturally occurring radioactive material (NORM) because of its elevated concentration of natural radionuclides [14]. Additionally, it emits particles and gases with high levels of radon and hydrogen fluoride, one of the most toxic gaseous compounds, into the atmosphere [48–50]. Moreover, this estuary is polluted with large amounts of metals generated by acid mine drainage due to the Odiel and

Tinto Rivers, which drain the province of Huelva from north to south through the Iberian Pyrite Belt, one of the most important polymetallic sulphide mining areas in Europe [51,52]. Furthermore, two important industrial complexes called "Polo Químico de Promoción y Desarrollo de Huelva—Punta del Sebo" (IC1; Figure 1) and "Nuevo Puerto Palos de la Frontera" are both placed in the margin of the Odiel–Tinto Estuary (IC2; Figure 1). The principal Spanish producers of copper and fertiliser, along with a thermal power plant and an oil refinery, are among the most contaminating industries situated in these chemical complexes [3,53].

The sampling network, comprising 17 rain gauges, was strategically distributed at various distances from the sea and across different soil uses and human activities, including industrial, mining, urban, and agricultural waste areas. These rain gauges were situated at public institutions, private companies, and residential addresses. Moreover, both the wind and population centres were also considered to ensure that highly populated areas influenced by all major wind directions were included. Furthermore, due to the considerable size of the city of Huelva and its proximity to the phosphogypsum stacks, five rain gauges were installed to cover the entire city. The disposition of the rain gauges throughout the Huelva metropolitan area is depicted in Figure 1, with their main characteristics outlined in Table S1. As seen in Figure 1, the phosphogypsum stacks (FB) rain gauge is chosen as the central point of the affected area. Its UTM-30 coordinates, referenced with the ETRS89 reference system, are (x, y, z) 153073.3, 4130808.5, 6.5.

2.2. Sampling and Methodology

2.2.1. Rainwater Sampling and Hellman Rain Gauge Characteristics

Rainwater samples were collected using 17 Hellman rain gauges (DARRERA, Barcelona, Spain) during the period of January 2021 to December 2022 on an event basis. This period was chosen in order to make sure that every rain gauge was monitored for at least two complete hydrologic years. An event is classified as rainfall measuring at least 1mm following a dry period lasting a minimum 24 h.

The Hellman rain gauge with a circular collecting area of 200 cm^2 at a height of 1.5 m (World Meteorological Organisation standard) is made of plastic. Automatic rain gauges were not selected for rainwater sampling, as they discard the collected rainwater before a new rainfall event. The instrument includes an upper part with a limiter ring, a lower part, a collecting can, a holder, and a precipitation-measuring plastic vessel DIN 58667B (DARRERA, Barcelona, Spain), with a 0–10 mm scale in 1/10 mm increments. To prevent evaporation, the precipitation vessel is separated from the upper segment by an air chamber, and the exterior parts are made in pale grey that can be used on the outer surface of the rain gauge to reduce the thermal load. After an extended dry period, which is normal in the study area, it is crucial to thoroughly clean the rain gauge with deionised water and perform maintenance of before a rain event. This ensures that the composition of single-event samples can be reflected as wet-only deposition. After a rain event, rainwater was measured using graduated cylinder and collected in plastic bottles, and the rain gauges were thoroughly cleaned with deionised water. Samples were promptly collected after rainfall ended, typically the day after the event. In the laboratory, samples were filtered through 0.45 mm polypropylene membranes (Sigma-Aldrich, St. Louis, MO, USA) to eliminate insoluble particulate matter. Four replicates were conducted for each sample; two of them were acidified until they reached a pH below 2.5, and other two were unacidified, which were stored in a refrigerator at a temperature below 4 °C to maintain their chemical properties until analysis, which was conducted as soon as possible after sampling, typically within two weeks. In this study, a total of 612 rainwater samples, each up to 50 mL, were collected.

Concerning the trace elements monitored in this study, the quality of rainwater samples collected using the Hellman rain gauges are significantly impacted by numerous aspects (Text S1) [30]. Consequently, a quality score ranging from 1 to 5 (1 = poor, 5 = excellent) is assigned to each rain gauge in Table S1.

2.2.2. pH and Conductivity

The pH and conductivity (EC) of the rainwater samples were assessed within 24 h after collecting utilising a digital multimeter, specifically the LAQUA PC220 (HORIBA Advanced Techno Co., Ltd., Tokyo, Japan). To measure the pH and EC of the rainwater samples, the electrode was immersed in the samples and left there until the multimeter reached a stable pH measurement. The corresponding value at 25 °C was obtained by a temperature conversion of the results. The multimeter was calibrated daily using standard solutions of 4.01, 7.00, and 9.21 pH units as the evaluated rainwaters ranged from basic to acid, and using solutions of 147 $\mu S\ cm^{-1}$ and 1413 $\mu S\ cm^{-1}$ as these values encompassed the majority of the EC values of the rainwaters.

2.2.3. Major Anions and Cations

The concentration of major cations (Ca^{2+}, K^+, Mg^{2+}, and Na^+) in acidified samples were determined by Inductively Coupled Plasma–Optical Emission Spectroscopy (ICP-OES) with an Agilent 5110 (Agilent Technologies, Tokyo, Japan). This instrument operates within the wavelength range of 160–900 nm and utilises external and periodic calibration with concertation ranges of 0.1–100 ppm (K^+ and Na^+) and 0.1–500 ppm (Ca^{2+} and Mg^{2+}). The detection and quantification limits for these measurements were 0.1 ppm (Ca^{2+} and Mg^{2+}) and 0.5 ppm (K^+ and Na^+). To ensure calibration stability, the concentration of a 10 ppm standard solution was determined every 10 analyses, yielding a deviation of less than 10%. A subset comprising 10% of the samples was analysed in triplicate. Additionally, to verify the method's accuracy, an Agilent multi-element quality control standard (Number 5190–9418; Agilent Technologies, Tokyo, Japan) was employed, applicable for both EPA methods and other applications. The recovery rates were verified through periodic analyses of certified quality control samples (Number 5190–9418) interspersed within the analysis sequence with results ranging between 80% and 120%.

On the other hand, the concentrations of anions (Cl^-, F^-, NO_2^-, NO_3^-, PO_4^{3-}, and SO_4^{2-}) as well as NH_4^+ were determined in unacidified rainwater samples using the Metrohm automated ion chromatography system, model 883 BASIC IC PLUS (Metrohm AG, Herisau, Switzerland). Ion chromatography was employed to analyse aqueous samples containing ppm quantities of common anions [54]. Anion separation was conducted using a Metrosep A Supp 5 250/4.0 column (Metrohm AG, Herisau, Switzerland) with a flow rate of 0.7 $mL\ min^{-1}$ of a carbonate/bicarbonate eluent (3.2 mM Na_2CO_3 + 1.0 mM $NaHCO_3$). In contrast, NH_4^+ separation was performed on a Metrosep C4 250/4.0 column (Metrohm AG, Herisau, Switzerland) with an eluent composition of 4 mM tartaric acid + 0.75 mM dipicolinic acid at a flow of 1.0 $mL\ min^{-1}$. To ensure precise calibration, external standards prepared from commercial calibration standards at a concentration of 1000 mg/L were utilised. The calibration range for minor anions (F^-, NO_2^- and PO_4^{3-}) spanned from 0.05 to 25 ppm (0.1–25 ppm F^-, 0.05–25 ppm NO_2^-; 0.5–25 ppm PO_4^{3-}), while for major anions (Cl^-, NO_3^- and SO_4^{2-}) it ranged between 0.25 and 250 ppm (0.5–250 ppm Cl^-; 0.25–125 ppm NO_3^-; 0.5–250 ppm SO_4^{2-}). In each analytical sequence, calibration blanks were assessed. Moreover, 10% of the samples underwent triplication. Quality control standards were evaluated as well, with one standard positioned within the high concentration range and another at concentrations proximate to the method's quantification limits. The quantification limits for each analyte were established as follows: 0.1 ppm for F^-, 0.5 ppm for Cl^-, 0.05 ppm for NO_2^-, 0.25 ppm for NO_3^-, 0.5 ppm for PO_4^{3-}, and 0.5 ppm for SO_4^{2-}. The criteria for method validation were as follows: relative standard deviation (RSD) for the duplicate samples must be below 15%, and the deviation of the control standard values from the theoretical values must also be under 15%. Furthermore, five-point calibration curves for anions and cations were established using two certified multi-element ion chromatography standard solutions obtained from Sigma-Aldrich (St. Louis, MO, USA). All reagents, standards, and eluents were prepared with reagent-grade water (resistivity: 18.2 MΩ cm, total organic carbon concentrations: <10 μg L^{-1}) produced from an Elix 3/Milli-Q Element system (Millipore, Billerica, MA, USA). The method detection limits (MDLs) were estimated according to the guidelines set by the U.S. EPA in 40 CFR 136, Appendix B [55]. The recovery rates were assessed by conducting routine analyses of two certified multi-element ion chromatography standard solutions supplied by Sigma-Aldrich, which were systematically integrated into the sequence of analyses. The recorded results demonstrated a variation ranging from 80% to 120%. To maintain data quality, each sample was analysed in triplicate, with sample batches frequently interspersed with reference material and digestion blanks.

2.2.4. Trace Elements

Trace element (As, Ba, Cd, Co, Cr, Cu, Mn, Mo, Ni, Pb, Sr, V, and Zn) concentrations were determined in acidified samples by Inductively Coupled Plasma–Mass Spectrometry (ICP-MS) Agilent 7700 (Agilent Technologies, Tokyo, Japan) with SPS4 autosampler and collision cell (He mode). ICP-MS is a highly sensitive type of mass spectrometry that enables the determination of a wide range of elements, including trace elements (ppb) [56]. Molecular (polyatomic) ions are commonly formed in the inductively coupled plasma and can provoke interferences in ICP-MS. In this study, molecular ion elimination through kinetic energy discrimination (KED) was applied by adding 4.3 mL min^{-1} He gas flow in the collision cell (ORS) of the ICP-MS instrument. This method is commonly used in ICP-MS and has historically proven to be efficient. In particular, the specifications of the instrument used in this study (Agilent 7700 ICP-MS) showed an interference removal factor >30 (expressed as the ratio $^{59}Co/51ClO$). Further studies of the possible interferences for each analyte isotope and each potential molecular ion interferent were not conducted, since such fundamental ICP-MS studies were considered to be out of scope in this work. An internal solution containing Rh was added on-line to the samples to correct signal drifts. The calibration range was from 0.5 ppb to 250 ppb for all elements, and the quantification limit was 0.5 ppm. Internal quality controls (IQCs) were used according to the work instructions included in the Quality Manual according to ISO9001 and 14001 standards [57,58]. Various IQCs were implemented to confirm that the analytical procedure, from digestion to analysis, was conducted appropriately, enabling analytical chemists to verify the accuracy of the results. The laboratory quality controls used to determine the metals using ICP-Ms technique were the AccuTrace™ certified reference standards ICP-MS Quality Control Sample 1 (ICP-MS-QC1-1) and ICP-MS Quality Control Sample 2 (ICP-MS-QC2-1) supplied by AccuStandard®, Inc. (Berlin, Germany). To maintain data quality, each sample was analysed in triplicate, with sample batches frequently interspersed with reference material and digestion blanks.

2.2.5. Data Analyses and Spatial Variation

A descriptive statistical analysis was performed for each of the elements and stations studied, with outcomes expressed through measures of central tendency and dispersion. The normality of the variables was studied using the Kolmogorov–Smirnov test, considering, in all cases, a significance level of 95% ($p < 0.05$). In the case of the elements that followed a normal distribution, the mean and standard deviation were used, and, otherwise, median and interquartile range were used. The Statistical Package for the Social Sciences (SPSS) version 26.0 was used for data analysis.

Graphs were created representing the medians of the values collected for each of the elements per rain gauge location according to the distance to the reference station, as well as the one located in the phosphogypsum stacks (FB). In these graphs, by means of linear regression models, the corresponding line of adjustment has been included. The statistical package R version 2024.12.0+467 was used to create the graphs.

3. Results

The average annual precipitation during the studied period was 345.8 mm (Table S1), 260.5 mm in 2021 and 431.0 mm in 2022, quite a bit lower than the average annual precipitation of 505.6 mm [46]. Moreover, in November 2021, the studied area experienced its highest rainfall of 169 mm, followed by few successive weeks without any event (19 and 18 weeks in 2021 and 2022, respectively). In addition, the dominant wind direction in the study area was NW–NNW and SE–SSE (Figure 1).

3.1. pH and Conductivity

Rainwater characteristics differed significantly among the rain gauge locations (Table S2). Rainwater pH was slightly above 7 (alkaline pH) for all sampling points, with the exception of FB, FE, PU, RA, and SJ with pH values slightly below 7 (acid pH). The lowest pH values were obtained in the rain gauges located in the border (FE; 6.84) and especially inside (FB; 6.31) of phosphogypsum stacks (Table S2; Figure 2a). Rainwater EC ranged from 58.35 µS cm^{-1} in AL to 137.65 µS cm^{-1} in SJ (Table S2; Figure 2b), and these samples exhibited low EC in accordance with the WHO guidelines for drinking water quality [59].

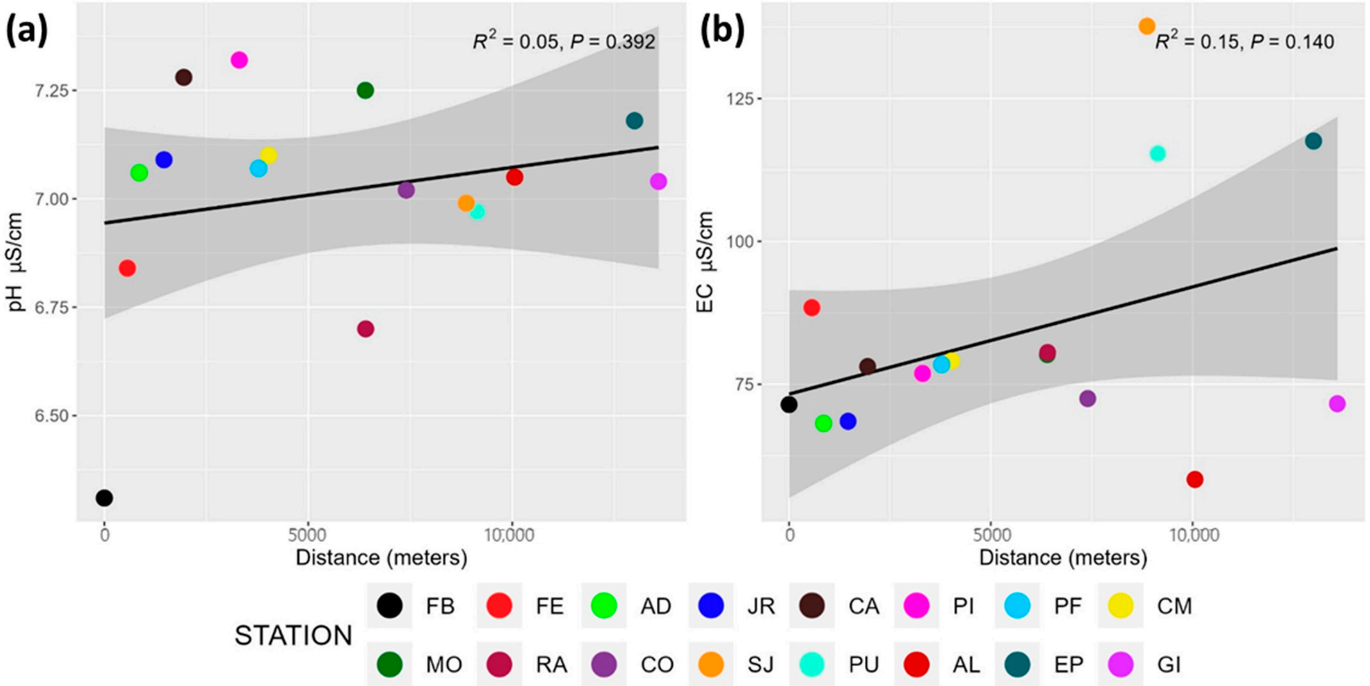

Figure 2. Scatter plots showing the distribution of (**a**) pH and (**b**) EC (µS cm^{-1}) in rainwater by rain gauge location. Sampling points are arranged by increasing distance (m) from phosphogypsum stacks (FB). Regression lines, standard error (grey shadow), correlation coefficients (R^2), and p-values are included in every plot.

The pH analysis shows a low relative standard deviation (5% of RSD on average), whereas the EC analysis displays a high RSD (100% on average), reflecting the significant chemical distinction across rain gauge locations. Skewness analysis is a measure of the asymmetry of the distribution. The positive skewness of the EC demonstrated asymmetric distributions and right-handed skewness. Moreover, pH displays a mean value slightly below zero, which showed asymmetric distributions and left-handed skewness (Table S2). The positive values of kurtosis in EC for most samples indicated sharp probability distributions.

3.2. Major Anions and Cations

The results of the analysis of ions, cations, and anions of rainwater are presented in Table S2. The concentration of ionic abundance (mg L^{-1}) displayed the overall pattern of $Cl^- > NO_3^- > SO_4^{2-} > PO_4^{3-} > F^- > NO_2^-$ for anions and $Ca^{2+} > Na^+ > K^+ > NH_4^+ > Mg^{2+}$ for cations. The samples were characterised by low Ca (4.73–14.84 mg L^{-1}), Cl^- (4.43–14.34 mg L^{-1}), K (1.32–6.35 mg L^{-1}), Mg (0.57–1.68 mg L^{-1}), Na (2.72–8.78 mg L^{-1}), NH_4^+ (0.10–3.94 mg L^{-1}), NO_3^- (2.33–8.21 mg L^{-1}), PO_4^{3-} (0.25–4.51 mg L^{-1}), and SO_4^{2-} (2.22–10.16 mg L^{-1}) values [59]. Meanwhile, F^- (0.03–2.94 mg L^{-1}) median is above the WHO guideline drinking value of 1.5 mg L^{-1} [59] and its concentration range is significantly influenced by the highest values in FB (2.66 mg L^{-1}) and FE (2.94 mg L^{-1}); without these (Table S2), the maximum value is 0.16 mg/L. Similarly, the NO_2^- median value obtained in SJ (0.33 mg L^{-1}) is the only one above the WHO guideline drinking value of 0.2 mg L^{-1} [59].

The variation in the major ion's concentration among the rain gauge locations revealed a high RSD (63% on average). Mean skewness and kurtoses values for each principal anion and cation are positive in all the locations studied with the exception of Ca^{2+}, indicating a rightward-extended tail (Table S2).

3.3. Trace Elements

On the other hand, a statistical summary of trace elements data in rainwater is shown in Table S2. The relative abundance in rainwater (µg L^{-1}) observed was Zn > Cu > Sr > Mn > Ba > Ni > As > Pb > V > Cr > Mo > Co > Cd. The samples were characterised by low As (0.50–3.06 µg L^{-1}), Ba (5.99+16.77 µg L^{-1}), Cd (0.25 µg L^{-1}), Co (0.25–0.50 µg L^{-1}), Cr (0.25–0.94 µg L^{-1}), Mn (5.02–35.80 µg L^{-1}), Mo (0.25–0.90 µg L^{-1}), Ni (0.76–6.21 µg L^{-1}), Pb (0.25–1.95 µg L^{-1}), and V (0.53–1.86 µg L^{-1}) values [59]. Moreover, Cu (2.78–199.13 µg L^{-1}) revealed a great influence in RA, although the values were in accordance with the WHO drinking guideline value (2000 µg L^{-1}) [59]. Similarly, the results revealed high Sr concentrations (11.36–32.54 µg L^{-1}), which do not pose a health risk and are significantly impacted by FB (Table S2). Moreover, high Zn (9.34–93.59 µg L^{-1}) median values were obtained, although the maximum values were in SJ, PU, RA, and FB (Table S2).

The trace metal concentrations analysis revealed a great RSD of over 100% on average. This is consistent with the significant natural variability among the infrequent and separated rainy events typical of a Mediterranean climate. The mean skewness and kurtoses values for each trace metal are positive across all the rain gauge locations, representing a tail extended to the right (Table S2).

3.4. Spatial Variation

Figures 2–5 illustrate how various parameters such as pH, EC, and elemental concentration change with the distance to the phosphogypsum stacks (FB). However, to truly understand the correlation, Pearson product–moment correlation coefficients (R^2) and p-values are contained within each plot.

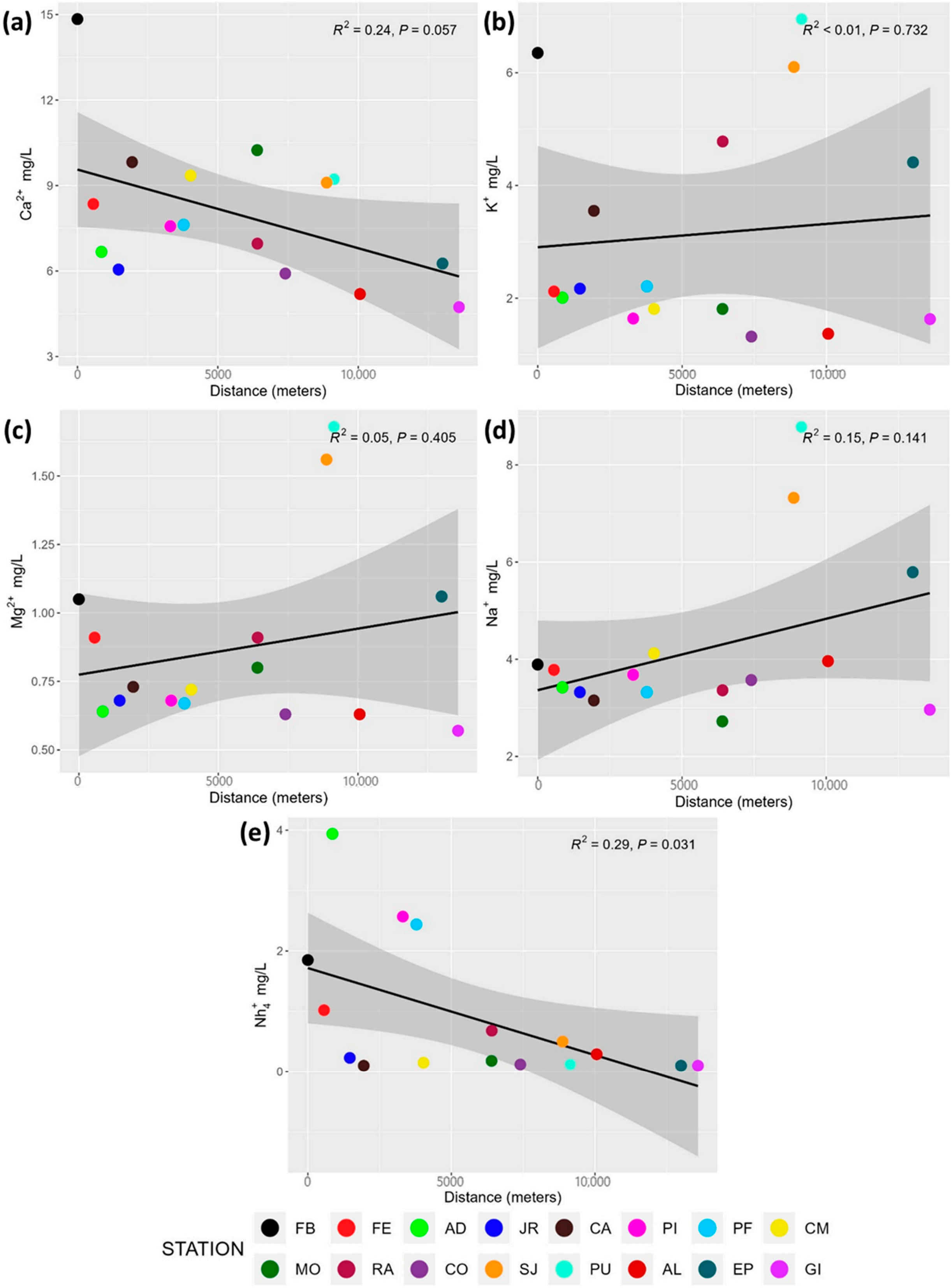

Figure 3. Scatter plots showing the distribution of major cation ((**a**) Ca^{2+}, (**b**) K^+, (**c**) Mg^2, (**d**) Na^+, and (**e**) $NH_4{}^+$) concentrations (mg L^{-1}) in rainwater by rain gauge location. Sampling points are arranged by increasing distance (m) from phosphogypsum stacks (FB). Regression lines, standard error (grey shadow), correlation coefficients (R^2), and *p*-values are included in every plot.

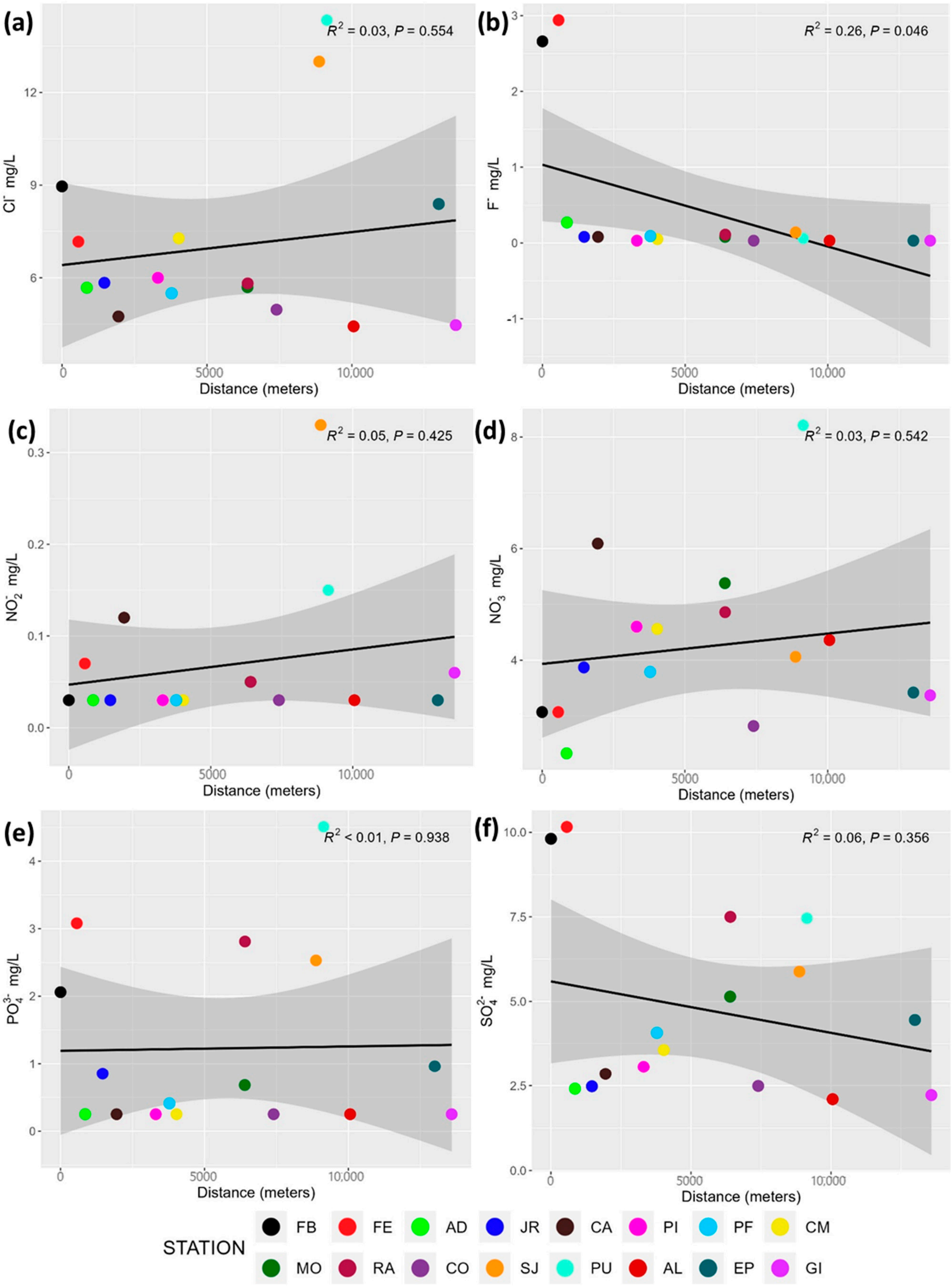

Figure 4. Scatter plots showing the distribution of major anion ((**a**) Cl^-, (**b**) F^-, (**c**) NO_2^-, (**d**) NO_3^-, (**e**) PO_4^{3-}, and (**f**) SO_4^{2-}) concentrations (mg L^{-1}) in rainwater by rain gauge location. Sampling points are arranged by increasing distance (m) from phosphogypsum stacks (FB). Regression lines, standard error (grey shadow), correlation coefficients (R^2), and *p*-values are included in every plot.

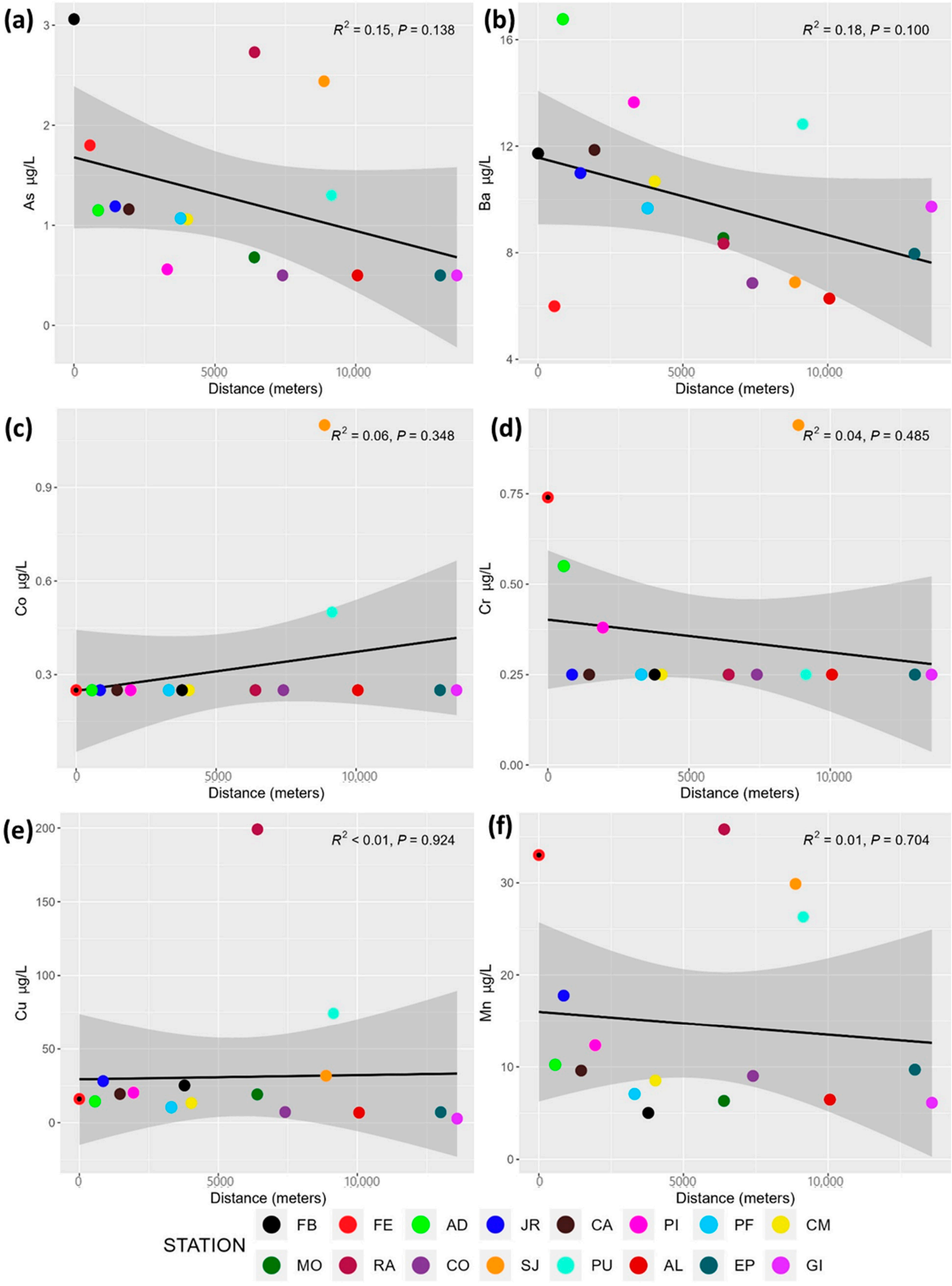

Figure 5. *Cont.*

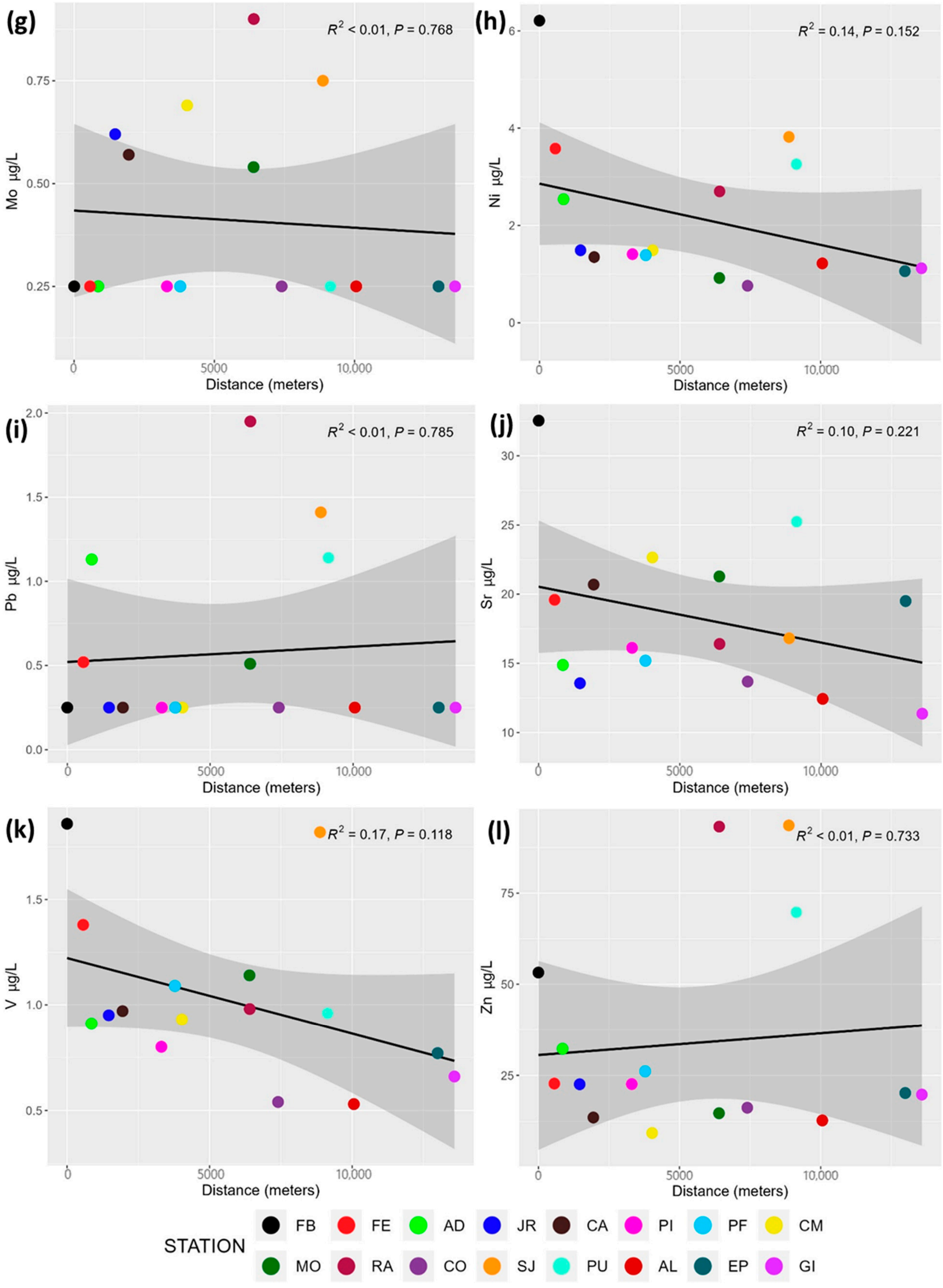

Figure 5. Scatter plots showing the variations of trace element ((**a**) As, (**b**) Ba, (**c**) Co, (**d**) Cr, (**e**) Cu, (**f**) Mn, (**g**) Mo, (**h**) Ni, (**i**) Pb, (**j**) Sr, (**k**) V, and (**l**) Zn) concentrations (µg L^{-1}) in rainwater by rain gauge location. Sampling points are arranged by increasing distance (m) from the phosphogypsum stacks (FB). Regression lines, standard error (grey shadow), correlation coefficients (R^2), and *p*-values are included in every plot.

4. Discussion

The influence of the phosphogypsum stacks on rainwater fallen in the Huelva metropolitan area was assessed through pH and EC measurements, the concentration of major anions (Cl^-, F^-, NO_2^-, NO_3^-, PO_4^{3-}, and SO_4^{2-}), major element content (Ca^{2+}, K^+, Mg^{2+}, Na^+, and NH_4^+), and trace element content (As, Cd, Co, Cr, Cu, Mn, Ni, Pb, Sr, V, and Zn) in the soluble fraction of rainwater collected in Hellmann rain gauges. In the south-western Mediterranean region, dryfall is dominant between consecutive rainy events [60]. This study revealed that the mean concentrations of F^-, Sr, and Ni were considerably higher and pH lower in rainwater collected in FB than these values in the WHO guidelines for drinking water quality [59]. Furthermore, most of the elements (As, Ca^{2+}, Cr, F^-, NH_4^+, Ni, PO_4^{3-}, SO_4^{2-}, Sr, and V) were quite a bit higher in FB compared to the other rain gauge locations, particularly when contrasted with unpolluted areas (MN). The findings indicated that the elements studied in the rainwater samples from the Huelva metropolitan area displayed consistent spatial variations. Most of these element concentrations decrease with distance to the phosphogypsum stacks (FB) and show a similar distribution pattern. The outcomes from this research are innovative and offer valuable insights into the exposure of residents living close to the phosphogypsum stacks.

4.1. pH and Conductivity

The mean median pH value of rainwater in the studied area was 7.03 (Table S2; Figure 2a), although the pH of unpolluted rainwater typically hovers around 5.6 due to the carbonate buffering effect of dissolved CO_2 in rain droplets [61]. The relatively elevated mean pH values observed in this area are not due to a lack of acidity in rainwater, but rather to the neutralisation of acidity in rainwater. The discrepancy may be due to the existence of sea-salt particles, which act as neutralising agents [33,62–64]. Elevated levels of sea-salts in rainwater have been previously documented in other locations, particularly for coastal regions [62–64]. According to previous studies, most phosphogypsum deposits are typically located in coastal zones close to the producing factories [65,66]. The key characteristic is the elevated levels of Ca^{2+}, Cl^-, Na^+, NO_3^-, Mg^{2+}, and SO_4^{2-}, indicating that neutralisation is the primary cause for the low acidity. As this study is located near the coast (Figure 1), sea-salt particles were the most dominant neutralising agents [62–64]. On the other hand, our lower pH values in rainwater compared with a similar study, which pH ranged from 7.0 to 7.5 [60–62], certainly result from rain acidity occurring by toxic acid gaseous compounds released into the atmosphere from the phosphogypsum stacks [49,50].

According to the pH (Table S2; Figure 2a), samples collected in rain gauges located close to phosphogypsum stacks (FB) revealed the minimum values (6.31), indicating acid pH values lower than the minimum value (6.5) recommend by the WHO guidelines for drinking water quality [59]. The low pH of rainwater ($pH < 6.5$) can impact the solubility of harmful elements like As, Cd, and Pb, potentially making rainwater a source of toxic metal(loid)s, which pose various health risks, including cancer and neurobehavioral disorders [59]. This acidity may be associated with the existence of acid-producing particulate matter (such as sulphide particles) in suspension and acid gaseous compounds (hydrogen fluoride) released to the atmosphere coming from the phosphogypsum stacks [49,50]. Phosphogypsum is mainly calcium sulphate hydrate ($CaSO_4 \cdot 2H_2O$), which is a waste product formed when phosphate rock is combined with sulphuric acid to produce phosphoric acid [15,16,21–23]. In addition, the results revealed an inverse correlation between SO_4^{2-} concentrations and pH values in rainwater (Figures 2a and 4f). Similar results were obtained in other studies conducted in areas affected by sulphide emissions [30,37,38,67]. Moreover, Figure 2a reveals the pH dependence with the distance to FB. At greater distances from the phosphogypsum stacks, the pH values increase due to these acid-producing minerals that are primarily neutralised by sea-salt particulate. Na^+ and Ca^{2+} denoted a similar pattern, indicating the transport of Cl^-, $SO_4{}^{2-}$, and $NO_3{}^-$, as well as buffering processes in accordance with other studies [33,62–64]. The R^2 and p-values indicate a slightly positive correlation ($R^2 = 0.05$) and a correlation that is not statistically significant (p-value = 0.392) between both variables.

Rainwater conductivity showed notable discrepancies among rain gauges (Table S2; Figure 2b). The elevated conductivity levels in most rainwater samples highlight the significant role of dissolved particles in the rainwater. In our case, the EC levels are influenced by the incidence of organic material from animals, primarily birds, and the nearby vegetation within the rain gauges [68]. This is the primary cause for the particularly high EC levels in SJ (137.65 µS cm^{-1}) > PU (115.35 µS cm^{-1}) > EP (117.55 µS cm^{-1}). Additional sources of inorganic contamination, such as heavy road traffic, dust, and ashes, are minor causes that affect the EC [69]. For these reasons, these rain gauges have the lowest quality score (SJ = 1; PU = 1; EP = 2). Similar EC values were obtained among the others rain gauges. The R^2 and p-values indicate a moderately positive correlation ($R^2 = 0.15$) and a slightly correlation (p-value = 0.140) between increases in EC levels and distance to the phosphogypsum stacks (Figure 2b).

4.2. Major Anions and Cations

Most precipitation events occurred in spring and autumn due to the study area having a Mediterranean climate. All ionic species vary throughout the year, although most ion concentrations were higher in the first rains of autumn. In accordance with previous studies conducted in Mediterranean areas [29,31,32,37,38,60,62,67], the highest concentration levels were observed at the beginning of rainy season (autumn) due to the accumulation of a large amount of soluble pollutants in the atmosphere after a long period without rain events, such as in summer, which were scavenged by the rain. Despite this, nitrite and nitrate were also high in spring. Since, during this season, the use of nitrogenous fertilisers was increased in the surrounding farm field, this could also contribute to increased $NO_3{}^-$ and $NO_3{}^-$ concentrations. A similar trend was obtained in other studies conducted near agricultural areas [29,31,32,60,62].

The major ion composition (Table S2) of rainwater in the Huelva metropolitan area was generally similar to that documented previously for other locations of Huelva province, except for F^- [37,38]. Variations can be attributed to different meteorological factors during the examination periods, as well as local factors such as the proximity and orientation to most important contamination sources, the effect of marine factors, dominant meteorological conditions, and other similar aspects. The outcomes showed the influence of the phosphogypsum stacks over rainwater chemical composition, increasing some of the major components such as Ca^{2+}, F^-, $PO_4{}^{3-}$, and $SO_4{}^{2-}$ (Table S2; Figures 3a and 4b,e,f). A downward trend in these ion concentrations in wet depositions was detected when the distance to the affected area increased. These findings are in accordance with previous studies, where the maximum concentration of these elements was detected in sediments close to phosphogypsum stacks [35] and also cumulated in nails of citizens residing near this waste [38]. This fact is greatly influenced by gases and particulate matter released from phosphogypsum stacks. Recent studies showed the presence of hydrogen fluoride (HF) in the air of Huelva city, attributed to emissions from phosphogypsum stacks [49,50]. The F^- concentrations are a health concern and are greatly influenced by phosphogypsum stack proximity. FE achieved the highest value (2.94 mg L^{-1}) and FB a similar value (2.66 mg L^{-1}), which are above the WHO drinking guideline value of 1.5 mg L^{-1} [59]. Concentrations above this value carry an increased risk of dental fluorosis, and much higher concentrations lead to skeletal fluorosis that is associated with osteosclerosis, the calcification of tendons and ligaments, and bone deformities [59]. Although the concentration falls with increased distance from the phosphogypsum stacks, the emissions of this gas are demonstrated, which is considered as one of the most harmful gaseous compounds present in the air [49,50]. The findings indicate that phosphogypsum stacks are the primary anthropogenic source of F^- contamination. Furthermore, phosphogypsum ($CaSO_4{\cdot}2H_2O$) is mainly composed of Ca^{2+} and $SO_4{}^{2-}$, and it contains some residual phosphorous originating from the phosphate rock utilised in the production process of phosphoric acid [15,16,21–23]. The occurrence of these elements in the phosphogypsum stacks indicates an increase in the air of these kinds of airborne particulates during dry and windy conditions [30,37,38,67], which would subsequently lead to a rise in Ca^{2+}, $PO_4{}^{3-}$, and $SO_4{}^{2-}$ concentration in rainwater (Figures 3a and 4e,f). Since, over the years, south-westerly to north-westerly winds prevail along the estuary, the transport of Ca^{2+}, $PO_4{}^{3-}$, and $SO_4{}^{2-}$ from phosphogypsum stacks is possible. Moreover, Ca^{2+} concentration is also related to sea-salt particles from the proximity to the ocean, as occurred in previous similar studies conducted close to the sea [3,62–64]. However, calcium also probably comes from the soil, as the Huelva metropolitan area is rich in calcareous soils [46]. In addition, $PO_4{}^{3-}$ is related to organic dirt from animals, mainly birds, and the surrounding vegetation inside the rain gauges [68]. Furthermore, these major ion concentrations are inversely correlated (negative correlation) to the distance from the phosphogypsum stacks, revealing that these are the main pollution source of as F^- and $SO_4{}^{2-}$ (Figure 4b,f). According to R^2 and p-values, the concentration of every major ion component in relation to distance can be ranked in the following order: $F^- > Ca^{2+} > Na^+ > SO_4{}^{2-} > Mg^{2+} > NO_2{}^- > NO_3{}^- > Cl^- > K^+ > PO_4{}^{3-} > NH_4{}^+$. The low R^2 values, ranging from 0.01 to 0.25 in absolute terms, indicate weak statistical correlations between each pair of variables. Moreover, the observed low significance levels, with p-values ranging from 0.046 to 0.911, validate that the possibility of the correlation is negligible.

On the other hand, positive correlations between Cl^-, K^+, Mg^{2+}, Na^+, $NO_2{}^-$, and $NO_3{}^-$ concentrations and distance were found (Figures 3b–d and 4a,c,d). This situation may come from the fact that the other major components have both a sea influence and a crustal/agricultural origin, as revealed by previous studies [35,62–64]. Consequently, salts dissolved in rainwater come from marine aerosol and continental sources, both natural and anthropogenic. Considering that the majority of rain gauge locations are positioned close to the coast (Figure 1), the distances shown in Figure 3 are also linked to the proximity to the coast. This strong sea influence on rainwater concentrations for Cl^-, K^+, Mg^{2+}, and Na^+ is due to the absence of sources for these major anions and elements in the vicinity of the rain gauge locations, as well as the proximity to the sea. This might explain the positive correlation observed for Cl^-, K^+, Mg^{2+}, and Na^+, as well as the occurrence of Ca^{2+} and $SO_4{}^{2-}$ inland, in accordance with other studies [30,35,62–64,67,70,71]. Additionally, the high values of Ca^{2+}, Cl^-, K^+, Mg^{2+}, and Na^+ at the control rain gauge location (MN), which is located in an unpolluted area close to the Atlantic Ocean (less than 1 km), denotes a great influence by sea-salts and aerosols (Table S2). The chemical profile of the marine source remained consistent in the region for the entire duration of the study.

However, animal and vegetation dusts and fertilisers from the surrounding farmland are generally nitrogen-rich natural and anthropogenic sources [72] and may be responsible for the origin of $NO_2{}^-$ and $NO_3{}^-$. Furthermore, the high content for all the major anions and elements studied, with the exception of F^- and $SO_4{}^{2-}$, in SJ, PU, and EP (Table S2), could be attributed to the debris in the rain gauge, which is likely caused by birds and nearby vegetation [68], which were the cause of the rain gauge locations with the lowest quality score (Table S1). These results are in accordance with the EC results, which showed the highest EC values (Table S2) and the lowest quality scores (Table S1). This fact is proven in SJ, placed at 8.9 km from phosphogypsum stacks, with high concentrations of major ions. Moreover, in the northeast of Huelva city an industrial area "Polígono Tartessos" is located that hosts a pulp and paper industry Empresa Nacional de Celulosas (Ence)-Energía y Celulosa, S.A. This facility has been in operation for over 70 years, and pulp and paper production was finally closed in 2014; it currently produces renewable energy with agroforestry biomass. The proximity of this area, situated 1 km southeast of San Juan city (aligned with the predominant wind direction), in conjunction with its closeness to the phosphogypsum stacks, make the rain gauge location of SJ mostly susceptible to the incidence of organic dust and even heavy metals [73]. With regard to NH_4^+, it may originate either from bird and vegetation debris or from combustion processes in the power plant [73].

4.3. Trace Elements

The source of pollutant emissions might be causing the seasonal variation in trace metal concentrations during different rainfall events. Rainfalls after dry periods showed high metal concentrations, whereas rainfalls that continued for several days had lower metal concentrations. The relative abundance of trace elements in rainwater is determined by their evaporation rate, their concentration within the samples, and their solubility (Table S2).

The results revealed the influence of the phosphogypsum stacks over rainwater quality, increasing some of the trace elements such as As, Ni, Sr, and V (Table S2; Figure 5a,i,j). As the distance from the affected area increases, a decline in the concentrations of most toxic metal(loid)s in wet depositions was observed. The chemical profile of rainwater samples in the studied area exhibits varying concentrations of trace elements depending on the volume of rainfall, the trajectory of the rainfront, and the interval between the precipitation events [74]. The trace element concentration in the rainwater of the Huelva metropolitan area was quite high compared with the MN location, which is an unpolluted area (Table S2), and other studies conducted in rural areas [29,31–34]. Some of the trace elements showed a possible correlation between their concentrations and the distance from the phosphogypsum stacks considering R^2 and p values (Figure 5). The correlations decreased in the following order: Ba > V > As > Ni > Sr > Co > Cr > Mn > Zn > Mo > Pb > Cu. The low values of R^2, in the range of 0.01–0.18 in absolute amounts, reveal weak statistical relationships between every pair of variables, as occurred with major components. In addition, the low significance levels observed (p-values ranged from 0.100 to 0.924) suggest a slight likelihood of correlation.

In this study, only Co, Cu, Pb, and Zn correlations with the distance to the phosphogypsum stacks are positive (Figure 5c,e,i,l), with the rest being negative (As, Ba, Cr, Mn, Mo, Ni, Sr, and V). The elements that were negatively correlated appear to be associated with the phosphogypsum stacks due to the fact that the mean concentration decreased with distance (Figure 5a,b,d,f–h,j,k). These trace elements are contained in phosphogypsum stacks [15,16] and, according to previous studies [21–23], they are widely geo-available due to the weathering they suffered. In addition, previous studies revealed that the marsh pollution signature near the phosphogypsum stacks was characterised by 20 elements, including As, Mn, Mo, Ni, Sr, and V [12]. Similarly, other research concluded that Huelva residents living near the phosphogypsum stacks had the maximum cumulated levels of As, Ni, and Sr in nails [13]. Furthermore, very high Ni concentration is a health concern and is greatly influenced by phosphogypsum stack proximity, achieving the highest mean value in FB (86.85 $\mu g\ L^{-1}$), which is strongly above the WHO guideline drinking value of 70 $\mu g\ L^{-1}$ [59]. The critical effect for the risk characterisation of chronic exposure to nickel is reproductive and developmental toxicity [5]. Moreover, there is strong metallurgical activity close to the phosphogypsum stacks located in “Polo Químico de Promoción y Desarrollo de Huelva—Punta del Sebo” (IC1; Figure 1) chemical industry complexes, which release As, Cr, Mn, and other trace elements in accordance with previous research [39–45]. These previous studies on the air quality in the city of Huelva attributed the majority of the Sr and V emissions, with the crude oil refinery located in the “Nuevo Puerto Palos de la Frontera” (IC2; Figure 1) industrial complex identified as the primary source [39–45]. Additionally, this spatial variation may be the result of air input contaminated with industrial emissions from both the fertiliser factory and phosphogypsum stacks, combined with the closeness to the industrial complexes and the prevailing northwest wind direction; Huelva city is exposed to the significant atmospheric deposition of these elements [15,16,21,22,39–45].

In contrast, correlations for Co, Cu, Pb, and Zn were positively correlated with the distance to the phosphogypsum stacks. The elements Cu, Pb, and Zn are most likely associated with the heavy chemical industry complexes located in the vicinity of the city. This inference is substantiated by the observation that the highest concentrations of these elements were recorded at RA, followed by PU, which represents the sampling points nearest to these industrial complexes. The enrichment factors of Cu, Pb, and Zn indicated significant anthropogenic influences due to industrial emissions, as revealed by similar studies conducted in highly polluted areas in China [75] and Bangladesh [76]. Furthermore, similar results were reached in earlier studies conducted in Huelva province (Rio Tinto Mining District), which shown higher deposition fluxes in the soluble fraction of Cu, Pb, and Zn associated with mining/metallurgical activities [37,38]. The spatial variation of Cu, Pb, and Zn is in accordance with previous studies [12,13], which identified the distinct sediment pollution signatures in the Odiel–Tinto Estuary and the internal cumulated dose of harmful metal(loid)s in Huelva residents from diverse sources, revealing the highest concentration close the chemical complexes (Figure 1). Moreover, other studies on the air quality of Huelva city revealed that Cu and Pb emissions are linked to a copper smelter situated southeast of the city located in the “Nuevo Puerto Palos de la Frontera” (IC2; Figure 1) [39–45]. The literature suggests that Pb exposure can potentially lead to respiratory, neurological, digestive, cardiovascular, and urinary disorders [59]. Moreover, long-term exposition to copper can cause dizziness, headaches, and other severe diseases, such as kidney and liver damage. Breathing in copper dusts, sprays, or crystals can irritate your nose and throat [59]. In addition, elevated Zn levels pose no significant health risk and are heavily impacted by the material of the rain gauge [59].

As happens in the case of major components, rain gauge locations with the minimum quality score (SJ, PU, and EP) typically exhibit high levels for most trace elements. This fact denotes that dirt from other pollution sources, like heavy road traffic, dust, ashes, and bird droppings are factors that greatly impact rainwater chemical composition [68]. In addition, a thermal power plant is located in an industrial area “Polígono Tartessos” near the SJ rain gauge, which produces a significant amount of greenhouse gas emissions, dust, and trace elements, such as Co, Cr, and Zn. This situation might be crucial in understanding the localised increase in the concentration of these elements at this particular site, particularly cobalt, which is reduced by two orders of magnitude at other rain gauge locations. In this area, phosphogypsum stacks are the predominant source mixed with other secondary sources located inside the city of San Juan (SJ). This combination of the phosphogypsum stacks and local emission sources results in a mixture of trace elements originating from both natural sources (such as vegetation and animal dirt) and human activities (including power plant and traffic emissions).

More studies are needed to link the specific contribution of metals from the phosphogypsum stacks from different sources (trophic chain, water geochemistry, direct air resuspension, dust deposition from rain) to the pollution load of the Huelva Estuary to study its association with local morbidity and mortality.

5. Conclusions

The results of this study reveal certain spatial variability on the chemical profile of the rainwater samples collected in the Huelva metropolitan area. An enrichment of potentially harmful metal(loid)s such as As, Ca^{2+}, Cr, F^{-}, Ni, $PO_4{}^{3-}$, $SO_4{}^{2-}$, Sr, and V were detected in the soluble fraction in areas close to the phosphogypsum stacks. Only in the rain gauges near the phosphogypsum stacks did the found levels of pH, F^{-}, and Ni significantly surpassed the guideline values for drinking water quality by the WHO. In addition, other main pollution sources were identified in the studied area: a regional source comprising sea-salt particles and the aerosols from the Atlantic Ocean and Odiel–Tinto Estuary (marine factors: Ca^{2+}, Cl^{-}, K^{+}, Mg^{2+}, and Na^{+}) and a local source from the chemical complexes (industrial emissions: Co, Cu, Pb, and Zn). Moreover, phosphogypsum stacks are predominantly situated along coastal areas around the world, rendering the marine influence a common factor among all such deposits. However, other local emission factor might influence the rainwater chemistry profile. This research serves as a crucial initial step in comprehending the distribution patterns of harmful metal(loid) concentrations in rainwater and raises significant questions about the effect of the phosphogypsum stacks and the chemical industries on the environment and health in this area. These results revealed the real impact of the identified pollution sources in the quality of the rainwater of the Huelva metropolitan area, especially the areas closest to the phosphogypsum stacks. The influence of the phosphogypsum stacks is apparent in the sampling locations exposed to dust-bearing winds downwind of the area. This suggests that phosphogypsum stacks are the primary source of hazardous elements (As, Cr, F^{-}, Ni, $PO_4{}^{3-}$, and $SO_4{}^{2-}$), which could potentially have adverse environmental effects on the nearby ecosystem, and the population situated in the prevailing wind directions. Also, our results might be useful to supplement the data of the proportion of pollution sources in the study area. Despite this, more studies in other similar study areas are warranted before addressing environmental policy implications. This study could help as an initial step in evaluating the influence of the RESTORE 2030 restoration plan for the Odiel–Tinto Estuary. These chemical patterns might also be used as a reference to assess the effect of upcoming interventions on existing contamination sources in other similarly contaminated areas. Furthermore, long-term monitoring post restoration could identify changes and trends, offering a more in-depth understanding of the environmental and health implications in the study area.

Supplementary Materials: The following supporting information can be downloaded at: https://www.mdpi.com/article/10.3390/su17073102/s1, Table S1. Main characteristics of the weather stations; Table S2. Descriptives.

Author Contributions: Conceptualization, M.C.-L. and R.R.-P.; methodology, M.C.-L. and R.R.-P.; software, V.S.-S.; validation, M.C.-L. and R.R.-P.; formal analysis, V.S.-S.; investigation, M.C.-L.; resources, J.A.; data curation, M.C.-L. and V.S.-S.; writing—original draft, M.C.-L.; writing—review & editing, M.C.-L., J.A. and R.R.-P.; Visualization, J.A. and R.R.-P.; Supervision, J.A.; Project administration, J.A. and R.R.-P.; Funding acquisition, J.A. All authors have read and agreed to the published version of the manuscript.

Funding: This research was funded by the Andalusian Government '2018 Special Action of the Andalusian Government: Support to the Huelva Phosphogypsum Experts Committee' and by Huelva University local funds to support research groups from 2018 to 2023.

Data Availability Statement: The original contributions presented in this study are included in the article/Supplementary Materials. Further inquiries can be directed to the corresponding author.

Acknowledgments: We want to thank Adrián Polonio, Irati Chasco, and Adrián Ruiz for sample collection support. We thank the management of the CEIP Hermanos Pinzón, CEIP Pedro Alonso Niño, CEIP Tierno Galván, CEIP Juan Ramón Jiménez, IES Diego Rodríguez, IES Odiel, IES Fuente Juncal, IES Saltes, IES Pintor Pedro Gómez, Casa del Mar, Railway Infrastructure Manager (ADIF), and Fertiberia for their collaboration. Special thanks to Ismael Dominguez Báez and Alba García Omedes in charge of the "El Portil-EP" rain gauge, who provided voluntary support in this collaborative project. The authors gratefully acknowledge the analysis support of the Research and Development Centre for Agri-Food Resources and Technologies (CIDERTA) in University of Huelva (Spain).

Conflicts of Interest: The authors declare the following financial interests/personal relationships, which may be considered as potential competing interests: Juan Alguacil reports that financial support was provided by Andalusian Government. If there are other authors, they declare that they have no known competing financial interests or personal relationships that could have appeared to influence the work reported in this paper.

References

1. Briffa, J.; Sinagra, E.; Blundell, R. Heavy metal pollution in the environment and their toxicological effects on humans. *Heliyon* **2020**, *6*, e04691. [CrossRef]
2. Nieto, J.M.; Sarmiento, A.S.; Olías, M.; Canovas, C.R.; Riba, I.; Kalman, J.; Delvalls, T.A. Acid mine drainage pollution in the Tinto and Odiel rivers (Iberian Pyrite Belt, SW Spain) and bioavailability of the transported metals to the Huelva Estuary. *Environ. Int.* **2020**, *33*, 445–455. [CrossRef] [PubMed]
3. Torre, B.M.; Borrero-Santiago, A.R.; Fabbri, E.; Guerra, R. Trace metal levels and toxicity in the Huelva Estuary (Spain): A case study with comparisons to historical levels from the past decades. *Environ. Chem. Ecotox.* **2019**, *1*, 12–18. [CrossRef]
4. Alguacil, J.; Ballester, F.; Donado-Campos, J.; Pollán, M.; Rodríguez-Artalejo, F. *Dictamen Realizado Por Encargo Del Defensor Del Pueblo Andaluz Sobre El Exceso de Mortalidad y Morbilidad Detectado en Varias Investigaciones en La Ría de Huelva*; Grupo de Trabajo de la Sociedad Española de Epidemiología: Seville, Spain, 2014. Available online: https://www.defensordelpuebloandaluz.es/informe-epidemiologico-ria-de-huelva (accessed on 11 January 2025).
5. Benach, J.; Yasui, Y.; Borrell, C.; Rosa, E.; Pasarín, M.I.; Benach, N.; Español, E.; Martínez, J.M.; Daponte, A. Examining geographic patterns of mortality: The Atlas of mortality in small areas in Spain (1987–1995). *Eur. J. Public Health* **2003**, *13*, 115–123. [CrossRef] [PubMed]
6. López-Abente, G.; Aragones, N.; Ramis, R.; Hernandez-Barrera, V.; Perez-Gomez, B.; Escolar-Pujolar, A.; Pollan, M. Municipal distribution of bladder cancer mortality in Spain: Possible role of mining and industry. *BMC Public Health* **2006**, *6*, 17. [CrossRef]
7. Martínez-Beneito, M.A.; Botella-Rocamora, P.; Corpas-Burgos, F.; Vergara- Hernández, C.; Pérez-Panadés, J.; Perpiñán-Fabuel, H. *Atlas Nacional de Mortalidad en España (ANDEES)*; Fundación FISABIO y Dirección General de Salud Pública de la Generalitat Valenciana: Valencia, Spain, 2024. Available online: http://andees.fisabio.san.gva.es/ (accessed on 11 January 2025).
8. Aguilera, I.; Daponte, A.; Gil, F.; Hernández, A.F.; Godoy, P.; Pla, A.; Ramos, J.L. Urinary levels of arsenic and heavy metals in children and adolescents living in the industrialised area of Ria of Huelva (SW Spain). *Environ. Int.* **2010**, *36*, 563–569. [CrossRef]
9. Rodríguez-Barranco, M.; Lacasaña, M.; Gil, F.; Lorca, A.; Alguacil, J.; Rohlman, D.S.; González-Alzaga, B.; Molina-Villalba, I.; Mendoza, R.; Aguilar-Garduño, C. Cadmium exposure and neuropsychological development in school children in southwestern Spain. *Environ. Res.* **2014**, *134*, 66–73. [CrossRef]
10. Capelo, R.; Rohlman, D.S.; Jara, R.; García, T.; Viñas, J.; Lorca, J.A.; Contreras-Llanes, M.; Alguacil, J. Residence in an Area with Environmental Exposure to Heavy Metals and Neurobehavioral Performance in Children 9–11 Years Old: An Explorative Study. *Int. J. Environ. Res. Public Health* **2022**, *19*, 4732. [CrossRef]
11. Silva-Caicedo, R.F.; Contreras-Llanes, M.; Capelo, R.; Zumel-Marne, A.; García-Sevillano, M.Á.; Santos-Sánchez, V.; Alguacil, J. Impact of Fish, Mollusk and Seafood Consumption before Sample Donation on Urinary and Toenail Metal Levels in Workers Exposed to Heavy Metals. *Appl. Sci.* **2024**, *14*, 8174. [CrossRef]
12. Contreras-Llanes, M.; Santos-Sánchez, V.; Alguacil, J.; Castillo, J.M. Delineating distinct sediment pollution signatures from diverse sources in a heavily contaminated estuary near an area of high cancer and cardiovascular mortality. *Sci. Total Environ.* **2024**, *957*, 177715. [CrossRef]
13. Contreras-Llanes, M.; Alguacil, J.; Capelo, R.; Gómez-Ariza, J.L.; García-Pérez, J.; Pérez-Gómez, B.; Martin-Olmedo, P.; Santos-Sánchez, V. Internal cumulated dose of toxic metal(loid)s in a population residing near a Naturally Occurring Radioactive Material waste stacks and an industrial heavily polluted area with high mortality rates in Spain. *J. Xenobiot.* **2025**, *15*, 29. [CrossRef] [PubMed]
14. IAEA. *Application of the Concepts of Exclusion Exemption and Clearance*; Safety Standards Series; Safety Guide No. RS-G 17, STI/PUB/1202; International Atomic Energy Agency (IAEA): Vienna, Austria, 2004.

15. Contreras-Llanes, M.; Pérez-López, R.; Gázquez, M.J.; Morales, V.; Santos, A.; Esquivias, L.M.; Bolívar, J.P. Fractionation and fluxes of metals and radionuclides during the recycling process of phosphogypsum wastes applied to mineral CO_2 sequestration. *Waste Manag.* **2015**, *45*, 412–419. [CrossRef]
16. Contreras, M. Valorisation of Inorganic Waste for Obtaining Construction Materials. Ph.D. Thesis, University of Huelva, Huelva, Spain, 19 July 2017.
17. Scientific Committee of National Experts Coordinated from Huelva University About the RESTORE 2030 Plan. Technical Report on the Suitability of the RESTORE 20/30 Project as a Solution to the Problem of the Phosphogypsum Ponds and for the Recovery of the Marshes of the Tinto River Estuary. 2024. Available online: http://mesadelaria.es/documentos/Informe_280722_C_Expertos-Agosto2022.pdf (accessed on 20 June 2024).
18. Chopin, E.I.B.; Black, S.; Hodson, M.E.; Coleman, M.L.; Alloway, B.J. A preliminary investigation into mining and smelting impacts on trace element concentrations in the soils and vegetation around Tharsis, SW Spain. *Mineral. Mag.* **2003**, *67*, 279–288. [CrossRef]
19. Chopin, E.I.B.; Alloway, B.J. Trace element partitioning and soil particle characterisation around mining and smelting areas at Tharsis, Riotinto and Huelva, SW Spain. *Sci. Total. Environ.* **2007**, *373*, 488–500. [CrossRef]
20. López, M.; González, I.; Romero, A. Trace elements contamination of agricultural soils affected by sulphide exploitation (Iberian Pyrite Belt, SWSpain). *Environ. Geol.* **2008**, *54*, 805–818. [CrossRef]
21. Lieberman, R.N.; Izquierdo, M.; Córdoba, P.; Moreno Palmerola, N.; Querol, X.; Sánchez de la Campa, A.M.; Font, O.; Cohen, H.; Knop, Y.; Torres-Sánchez, R.; et al. The evolution of brines from phosphogypsum deposits in Huelva (SW Spain) and its environmental implications. *Sci. Total Environ.* **2020**, *700*, 134444. [CrossRef]
22. Pérez-López, R.; Nieto, J.M.; López-Coto, I.; Aguado, J.L.; Bolívar, J.P.; Santisteban, M. Dynamics of contaminants in phosphogypsum of the fertilizer industry of Huelva (SW Spain): From phosphate rock ore to the environment. *Appl. Geochem.* **2010**, *25*, 705–715. [CrossRef]
23. Rentería-Villalobos, M.; Vioque, I.; Mantero, J.; Manjón, G. Radiological, chemical and morphological characterizations of phosphate rock and phosphogypsum from phosphoric acid factories in SW Spain. *J. Hazard. Mater.* **2010**, *181*, 193–203. [CrossRef] [PubMed]
24. Pumlee, G.S.; Morman, S.A. Mine wastes and human health. *Elements* **2011**, *7*, 399–404. [CrossRef]
25. Brotons, J.M.; Diaz, A.R.; Sarria, F.A.; Serrato, F.B. Wind erosion on mining waste in southeast Spain. *Land Degrad. Dev.* **2010**, *21*, 196–209. [CrossRef]
26. Csavina, J.; Field, J.; Taylor, M.P.; Gao, S.; Landázuri, A.; Betterton, E.A.; Sáez, A.E. A review on the importance of metals and metalloids in atmospheric dust and aerosol from mining operations. *Sci. Total Environ.* **2012**, *433*, 58–73. [CrossRef]
27. Taylor, M.P.; Mackay, A.K.; Hudson-Edwards, K.A.; Holz, E. Soil Cd, Cu, Pb and Zn contaminants around Mount Isa city, Queensland, Australia: Potential sources and risks to human health. *Appl. Geochem.* **2010**, *25*, 841–855. [CrossRef]
28. Zota, A.; Willis, R.; Jim, R.; Norris, G.A.; Shine, J.P.; Duvall, R.M.; Schaider, L.A.; Spengler, J.D. Impact of mine waste on airborne respirable particulates in northeastern Oklahoma, United States. *J. Air Waste Manag. Assoc.* **2009**, *59*, 1347–1357. [CrossRef] [PubMed]
29. Al-Khashman, O.A. Study of chemical composition in wet atmospheric precipitation in Eshidiya area, Jordan. *Atmos. Environ.* **2005**, *39*, 6175–6183. [CrossRef]
30. Alcolea, A.; Fernández-López, C.; Vázquez, M.; Caparrós, A.; Ibarra, I.; García, C.; Zarroca, M.; Rodríguez, R. An assessment of the influence of sulfidic mine wastes on rainwater quality in a semiarid climate (SE Spain). *Atmos. Environ.* **2015**, *107*, 85–94. [CrossRef]
31. André, F.; Jonard, M.; Ponette, Q. Influence of meteorological factors and polluting environment on rain chemistry and wet deposition in a rural area near Chimay, Belgium. *Atmos. Environ.* **2007**, *41*, 1426–1439. [CrossRef]
32. Avila, A.; Alarcón, M. Relationship between precipitation chemistry and meteorological situations at a rural site in NE Spain. *Atmos. Environ.* **1999**, *33*, 1663–1677. [CrossRef]
33. Pelicho, A.F.; Martins, L.D.; Nomi, S.N.; Solci, M.C. Integrated and sequential bulk and wet-only samplings of atmospheric precipitation in Londrina, South Brazil (1998–2002). *Atmos. Environ.* **2006**, *40*, 6827–6835. [CrossRef]
34. Seto, S.; Hara, H. Precipitation chemistry in western Japan: Its relationship to meteorological parameters. *Atmos. Environ.* **2006**, *40*, 1538–1549. [CrossRef]
35. Zeng, J.; Han, G.; Wu, Q.; Qu, R.; Ma, Q.; Chen, J.; Mao, S.; Ge, X.; Wang, Z.; Ma, Z. Significant influence of urban human activities and marine input on rainwater chemistry in a coastal large city, China. *Water Res.* **2024**, *257*, 121657. [CrossRef]
36. Eriksson, E. Composition of atmospheric precipitation. I: Nitrogen compounds. *Tellus* **1952**, *4*, 215–232. [CrossRef]
37. Castillo, S.; de la Rosa, J.D.; Sánchez de la Campa, A.M.; González-Castanedo, Y.; Fernández-Caliani, J.C.; Gonzalez, I.; Romero, A. Contribution of mine wastes to atmospheric metal deposition in the surrounding area of an abandoned heavily polluted mining district (Rio Tinto mines, Spain). *Sci. Total Environ.* **2013**, *449*, 363–372. [CrossRef] [PubMed]

38. Castillo, S.; de la Rosa, J.D.; Sánchez de la Campa, A.M.; González-Castanedo, Y.; Fernández-Camacho, R. Heavy metal deposition fluxes affecting an Atlantic coastal area in the southwest of Spain. *Atmos. Environ.* **2013**, *77*, 509–517. [CrossRef]
39. Alastuey, A.; Querol, X.; Plana, F.; Viana, M.; Ruiz, C.R.; Sanchez de la Campa, A.; de la Rosa, J.; Mantilla, E.; García dos Santos, S. Identification and chemical characterization of industrial particulate matter sources in southwest Spain. *J. Air Waste Manag. Assoc.* **2006**, *56*, 993–1006. [CrossRef] [PubMed]
40. Chen, B.; Stein, A.F.; Castell, N.; González-Castanedo, Y.; Sánchez de la Campa, A.M.; de la Rosa, J.D. Modeling and evalua-tion of urban pollution events of atmospheric heavy metals from a large Cu-smelter. *Sci. Total Environ.* **2016**, *539*, 17–25. [CrossRef] [PubMed]
41. González-Castanedo, Y.; Moreno, T.; Fernández-Camacho, R.; Sánchez de la Campa, A.M.; Alastuey, A.; Querol, X.; de la Rosa, J. Size distribution and chemical composition of particulate matter stack emissions in and around a copper smelter. *Atmos. Environ.* **2014**, *98*, 271–282. [CrossRef]
42. Querol, X.; Alastue, A.; de la Rosa, J.; Sánchez-de-la-Campa, A.; Plana, F.; Ruiz, C.R. Source apportionment analysis of atmospheric particulates in an industrialised urban site in southwestern Spain. *Atmos. Environ.* **2002**, *36*, 3113–3125. [CrossRef]
43. Sánchez de la Campa, A.M.; de la Rosa, J.; Querol, X.; Alastuey, A.; Mantilla, E. Geochemistry and origin of PM10 in the Huelva region, southwestern Spain. *Environ. Res.* **2007**, *103*, 305–316. [CrossRef]
44. Sánchez de la Campa, A.M.; Sánchez-Rodas, D.; González Castanedo, Y.; de la Rosa, J.D. Geochemical anomalies of toxic elements and arsenic speciation in airborne particles from Cu mining and smelting activities: Influence on air quality. *J. Hazard. Mater.* **2015**, *291*, 8–27. [CrossRef]
45. Sánchez de la Campa, A.M.; Sánchez-Rodas, D.; Alsioufi, L.; Alastuey, A.; Querol, X.; de la Rosa, J.D. Air quality trends in an industrialised area of SW Spain. *J. Clean. Prod.* **2018**, *186*, 465–474. [CrossRef]
46. Achterberg, E.P.; Herzl, V.M.C.; Braungardt, C.B.; Millward, G.E. Metal behaviour in an estuary polluted by acid mine drainage: The role of particulate matter. *Environ. Pollut.* **2003**, *121*, 283–292. [CrossRef] [PubMed]
47. Silva, L.F.O.; Oliveira, M.L.S.; Crissien, T.J.; Santosh, M.; Bolivar, J.P.; Shao, L.; Dotto, G.L.; Gasparotto, J.; Schindler, M. A review on the environmental impact of phosphogypsum and potential health impacts through the release of nanoparticles. *Chemosphere* **2022**, *286*, 131513. [CrossRef] [PubMed]
48. López-Coto, I.; Mas, J.L.; Vargas, A.; Bolívar, J.P. Studying radon exhalation rates variability from phosphogypsum piles in the SW of Spain. *J. Hazard. Mater.* **2014**, *280*, 464–471. [CrossRef]
49. Torres-Sánchez, R.; Sánchez-Rodas, D.; Sánchez de la Campa, A.M.; Kandler, K.; Schneiders, K.; de la Rosa, J.D. Geochemistry and source contribution of fugitive phosphogypsum particles in Huelva, (SW Spain). *Atmos. Res.* **2019**, *230*, 104650. [CrossRef]
50. Torres-Sánchez, R.; Sánchez-Rodas, D.; Sánchez de la Campa, A.M.; de la Rosa, J.D. Hydrogen fluoride concentrations in ambient air of an urban area based on the emissions of a major phosphogypsum deposit (SW, Europe). *Sci. Total Environ.* **2020**, *714*, 136891. [CrossRef]
51. Leistel, J.M.; Marcoux, E.; Thieblemont, D.; Quesada, C.; Sanchez, A.; Almodovar, G.R.; Pascual, E.; Saez, R. The volcanic-hosted massive sulphide deposits of the Iberian Pyrite Belt. *Miner. Depos.* **1998**, *33*, 2–30. [CrossRef]
52. Pérez-López, R.; Millán-Becerro, R.; Basallote, M.D.; Carrero, S.; Parviainen, A.; Freydier, R.; Macías, F.; Cánovas, C.R. Effects of estuarine water mixing on the mobility of trace elements in acid mine drainage leachates. *Mar. Pollut. Bull.* **2023**, *187*, 114491. [CrossRef]
53. Blasco, J.; Sáenz, V.; Gómez-Parra, A. Heavy metal fluxes at the sediment–water interface of three coastal ecosystems from south-west of the Iberian Peninsula. *Sci. Total Environ.* **2000**, *247*, 189–199. [CrossRef]
54. Weiß, J. Ion chromatography—A review of recent developments. *Fresenius Z. Anal. Chem.* **1987**, *327*, 451–455. [CrossRef]
55. USEPA. *Appendix B to Part 136. Definition and Procedure for the Determination of the Method Detection Limit*; Revision 1.11. Fed. Regist. 49 (209), 43430. Also Referred to as "40 CFR Part 136"; Environmental Protection Agency: Washington, DC, USA, 1984.
56. Jenner, G.A.; Longerich, H.P.; Jackson, S.E.; Fryer, B.J. ICP-MS—A powerful tool for high-precision trace-element analysis in Earth sciences: Evidence from analysis of se-lected U.S.G.S. reference samples. *Chem. Geol.* **1990**, *83*, 133–148. [CrossRef]
57. *ISO 9001*; Quality Management Systems—Requirements. International Organization for Standardization: Geneva, Switzerland, 2015.
58. *ISO 14001*; Environmental Management Systems—Requirements with Guidance for Use. International Organization for Standardization: Geneva, Switzerland, 2015.
59. WHO. *Guidelines for Drinking-Water Quality*, 3rd ed.; Recommendations; World Health Organization: Geneva, Switzerland, 2008; Volume 1. Available online: https://iris.who.int/bitstream/handle/10665/204411/9789241547611_eng.pdf?sequence=1 (accessed on 11 January 2025).
60. Morales-Baquero, R.; Pulido-Villena, E.; Reche, I. Chemical signature of Saharan dust on dry and wet atmospheric deposition in the south-western Mediterranean region. *Tellus B Chem. Phys. Meteorol.* **2013**, *65*, 18720. [CrossRef]
61. Charlson, R.J.; Rodhe, H. Factors controlling the acidity of natural rainwater. *Nature* **1982**, *295*, 683–685. [CrossRef]

62. Al-Momani, I.F.; Tuncel, S.; Eler, Ü.; Örtel, E.; Sirin, G.; Tuncel, G. Major ion composition of wet and dry deposition in the eastern Mediterranean basin. *Sci. Total. Environ.* **1995**, *164*, 75–85. [CrossRef]
63. Dikaiakos, J.G.; Tsitouris, C.G.; Siskos, P.A.; Melissos, D.A.; Nastos, P. Rainwater composition in Athens, Greece. *Atmos. Environ.* **1990**, *241*, 171–176. [CrossRef]
64. Tuncer, B.; Bayer, B.; Yesilyurt, C.; Tuncel, G. Ionic composition of precipitation at the central Anatolia, Turkey. *Atmos. Environ.* **2001**, *35*, 5989–6002. [CrossRef]
65. Noli, F.; Sidirelli, M.; Tsamos, P. The impact of phosphate fertilizer factory on the chemical and radiological pollution of the surrounding marine area (seawater and sediments) in northwestern Greece. *Reg. Stud. Mar. Sci.* **2024**, *73*, 103458. [CrossRef]
66. Tayibi, H.; Choura, M.; López, F.A.; Alguacil, F.J.; López-Delgado, A. Environmental impact and management of phosphogypsum. *J. Environ. Manag.* **2009**, *90*, 2377–2386. [CrossRef]
67. Robles-Arenas, V.M.; Rodríguez, R.; García, C.; Manteca, J.I.; Candela, L. Sulphide-mining impacts in the physical environment: Sierra de Cartagena-La Unión (SE Spain) case study. *Environ. Geol.* **2006**, *51*, 47–64. [CrossRef]
68. Tranel, M.A.; Kimmel, R.O. Impacts of Lead Ammunition on Wildlife, the Environment, and Human Healthda—A Literature Review and Implications for Minnesota. In *Ingestion of Lead from Spent Ammunition: Implications for Wildlife and Humans*; Watson, R.T., Fuller, M., Pokras, M., Hunt, W.G., Eds.; The Peregrine Fund: Boise, ID, USA, 2009.
69. Wagner, S.; Funk, C.W.; Müller, K.; Raithel, D.J. The chemical composition and sources of road dust, and of tire and road wear particles–A review. *Sci. Total Environ.* **2024**, *926*, 171694. [CrossRef]
70. Custodio, E.; Llamas, M.R. *Hidrología Subterranea*; Omega: Barcelona, Spain, 1996; Volume I and II.
71. Todd, D.K.; Mays, L.W. *Groundwater Hydrology*, 3rd ed.; Wiley: Hoboken, NJ, USA, 2005.
72. Wakida, F.T.; Lerner, D.N. Non-agricultural sources of groundwater nitrate: A review and case study. *Water Res.* **2005**, *39*, 3–16. [CrossRef]
73. Raynor, G.S.; Hayes, J.V. Acidity and conductivity of precipitation on central Long Island, New York, in relation to meteorological variables. *Water Air Soil Pollut.* **1981**, *15*, 229–245. [CrossRef]
74. Granat, L. On the relation between pH and the chemical composition in atmospheric precipitation. *Tellus* **1972**, *24*, 550–560. [CrossRef]
75. Xing, J.; Song, J.; Yuan, H.; Wang, Q.; Li, X.; Li, N.; Duan, L.; Qu, B. Atmospheric wet deposition of dissolved trace elements to Jiaozhou Bay, North China: Fluxes, sources and potential effects on aquatic environments. *Chemosphere* **2017**, *174*, 428–436. [CrossRef] [PubMed]
76. Adhikari, S.; Zeng, C.; Zhang, F.; Adhikari, N.P.; Gao, J.; Ahmed, N.; Bhuiyan, A.Q.; Ahsan, A.; Khan, H.R. Atmospheric wet deposition of trace elements in Bangladesh: A new insight into spatiotemporal variability and source apportionment. *Environ. Res.* **2023**, *217*, 114729. [CrossRef]